LA-13164-MS

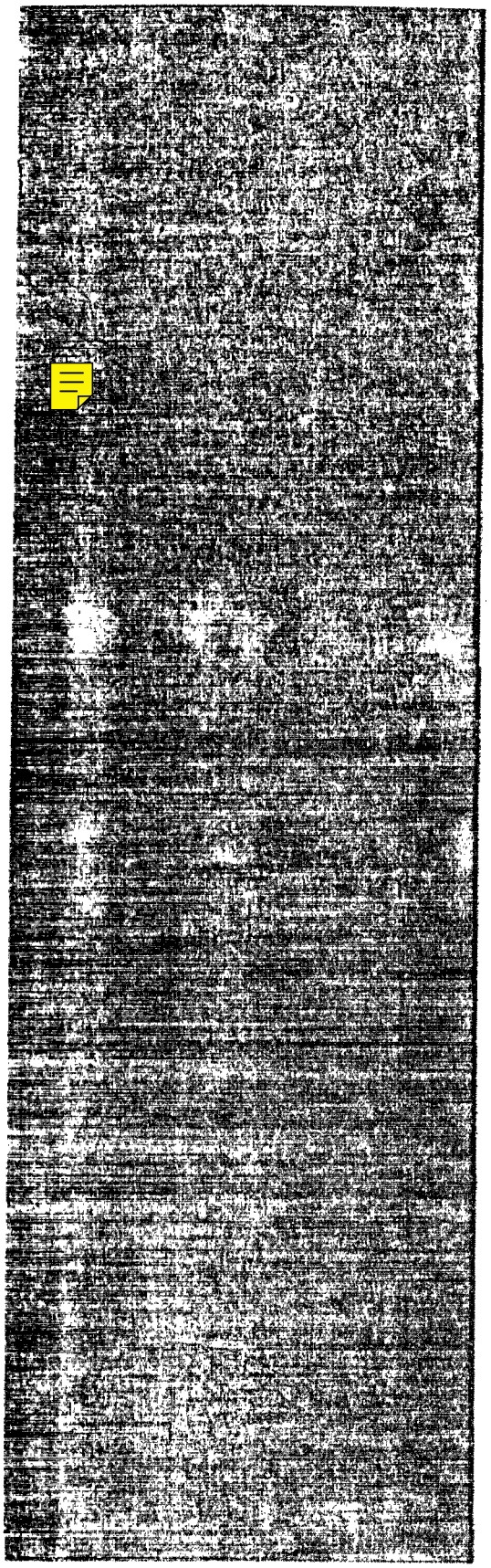

PBX 9501 High Explosive Violent Response/ Low Amplitude Insult Project: Phase I

Los Alamos
NATIONAL LABORATORY

Los Alamos National Laboratory is operated by the University of California for the United States Department of Energy under contract W-7405-ENG-36.

An Affirmative Action/Equal Opportunity Employer

This report was prepared as an account of work sponsored by an agency of the United States Government. Neither The Regents of the University of California, the United States Government nor any agency thereof, nor any of their employees, makes any warranty, express or implied, or assumes any legal liability or responsibility for the accuracy, completeness, or usefulness of any information, apparatus, product, or process disclosed, or represents that its use would not infringe privately owned rights. Reference herein to any specific commercial product, process, or service by trade name, trademark, manufacturer, or otherwise, does not necessarily constitute or imply its endorsement, recommendation, or favoring by The Regents of the University of California, the United States Government, or any agency thereof. The views and opinions of authors expressed herein do not necessarily state or reflect those of The Regents of the University of California, the United States Government, or any agency thereof. Los Alamos National Laboratory strongly supports academic freedom and a researcher's right to publish; as an institution, however, the Laboratory does not endorse the viewpoint of a publication or guarantee its technical correctness.

LA-13164-MS
UC-741
Issued: January 1997

PBX 9501 High Explosive Violent Response/ Low Amplitude Insult Project: Phase I

D.J. Idar
R.A. Lucht
R. Scammon
J. Straight
C.B. Skidmore

Los Alamos
NATIONAL LABORATORY
Los Alamos, New Mexico 87545

TABLE OF CONTENTS

ABSTRACT 1

I. INTRODUCTION 2

II. BACKGROUND 2

III. EXPERIMENTAL 3
A. SPIGOT GUN, PROJECTILE DESCRIPTION, AND POWDER CURVE TESTS 3
B. INERT TARGET DESCRIPTION 5
C. LIVE TARGET I DESCRIPTION 8
D. MILD STEEL BACKING PLATE DESCRIPTION 10
E. LIVE TARGET II DESCRIPTION 10
F. LIVE TARGET III DESCRIPTION 11

IV. DATA ANALYSIS AND RESULTS 12
A. LIVE TARGET TESTS 12
B. FERRITE SCOPE MEASUREMENTS 13
C. INSTRUMENTED TARGET RESULTS 16
D. PRELIMINARY ANALYSIS OF DAMAGED PBX 9501 35

V. MODELING PROBLEM SET-UP 41
A. APPROACH 41
B. IGNITION CRITERION 41

VI. MODELING ANALYSIS AND RESULTS 43
A. MATERIAL PROPERTIES AND CALIBRATION 43
B. CALCULATIONS 45
C. CARBON FOIL GAUGES.. 45
D. RADIAL PINDUCERS 47
E. REAR SURFACE PINDUCERS 48
F. IGNITION CRITERION 52

VII. EXPERIMETAL AND MODELING CONCLUSIONS 53
A. EXPERIMENTAL 53
B. MODELING 54

VIII. FUTURE OBJECTIVES 54
A. EXPERIMENTAL 54
B. MODELING 54

IX. ACKNOWLEDGMENTS 55
REFERENCES 57
DISTRIBUTION LIST 57

LIST OF TABLES

TABLE 1. POWDER CURVE PERFORMANCE RESULTS FOR LOW PRESSURE BARREL DESIGN 6-8
TABLE 2. POWDER CURVE PERFORMANCE RESULTS FOR HIGH PRESSURE BARREL DESIGN 9
TABLE 3. PBX 9501, LOT NUMBER HOL90C731, DENSITY REPORT 9
TABLE 4. TARGET DENT DATA MEASURED ON ASSEMBLED AND DISASSEMBLED TARGETS 13
TABLE 5. LIVE TARGET DATA SUMMARY 14
TABLE 6. DENSITY OF PBX 9501 CORE SAMPLES (g/cm^3), POST TEST 38
TABLE 7. MATERIAL PROPERTIES USED IN DYNA2D CALCULATIONS 44

LIST OF FIGURES

FIGURE 1. HOOP AND AXIAL STRAIN MEASUREMENTS OBTAINED FROM THE HIGH PRESSURE BARREL DESIGN FOR THE SPIGOT GUN 4
FIGURE 2. BORE PRESSURE AS A FUNCTION OF TIME FOR THE HIGH PRESSURE BARREL DESIGN 4
FIGURE 3. SPIGOT GUN AND PHOTODIODE VELOCITY SCREEN BOX 5
FIGURE 4. LIVE TARGET DESIGN I 10
FIGURE 5. LIVE TARGET DESIGN II, WITH 18 FOIL SWITCHES, ONE CARBON FILM GAUGE, AND 5 PINDUCERS 11
FIGURE 6. LIVE TARGET DESIGN III, WITH 14 FOIL SWITCHES, ONE THERMOCOUPLE, AND 7 PINDUCERS 12
FIGURE 7. FERRITE SCOPE MEASUREMENTS ON TARGET 3 FRAGMENTS, POST TEST, AFTER INTENTIONAL DETONATION OF PBX 9501 15
FIGURE 8. FERRITE SCOPE MEASUREMENTS ON TARGET 5 HARDWARE, POST TEST 15
FIGURE 9. KARL STAUDHAMMER'S FERRITE SCOPE DATA ON 304 SS 16
FIGURE 10. TARGET TEST 5 EXPERIMENTAL DATA AND DESIGN 17-18
FIGURE 11. TARGET TEST 6 EXPERIMENTAL DATA AND DESIGN 19-20
FIGURE 12. TARGET TEST 7 EXPERIMENTAL DATA AND DESIGN 21-24
FIGURE 13. TARGET TEST 9 EXPERIMENTAL DATA AND DESIGN 25-27
FIGURE 14. TARGET TEST 10 EXPERIMENTAL DATA AND DESIGN 28-31
FIGURE 15. ESTIMATED EXTENT OF PBX9501 REACTION AS A FUNCTION OF PROJECTILE VELOCITY 33
FIGURE 16. PBX 9501 TARGETS 3 AND 4 36
FIGURE 17. PBX 9501 TARGETS 6 AND 8 37
FIGURE 18. MACHINED SURFACES OF PBX 9501 FROM TARGET TEST 8, POST TEST 39
FIGURE 19. FRACTURE SURFACES OF PBX 9501 FROM TARGET TEST 8, POST TEST 40

FIGURE 20. LIGHT MICROSCOPE IMAGES OF A) COARSE HMX POWDER, B) THE MICRON SCALE OF THE IMAGES, C) SAMPLE OF PBX 9501 FROM TARGET 1, AND D) THE SAMPLE OF PBX 9501 FROM TARGET 9 40
FIGURE 21. PBX 9501, RECOVERED FROM SEMIVIOLENT REACTION OF TARGET TEST 9 41
FIGURE 22. DYNA2D MESH USED TO MODEL SPIGOT GUN PROJECTILE IMPACT ON PBX 9501 TARGET 42
FIGURE 23. DISTORTED DYNA2D MESH FOR TARGET TEST 4 (DF15-2330) 42
FIGURE 24. STRESS-STRAIN DATA FOR 304 STAINLESS STEEL (304 SS) 43
FIGURE 25. COMPARISON OF CALCULATED AND MEASURED FRONT DENT DEPTH AND REAR SURFACE DEFORMATION 44
FIGURE 26. AXIAL STRESS AT THE REAR SURFACE OF THE PBX 9501 AS A FUNCTION OF RADIAL OFFSET FROM THE CENTER LINE, TARGET TEST 5 (DF15-2347) 46
FIGURE 27. CARBON FOIL GAUGE DATA AND CALCULATIONS, TARGET TESTS 5 (DF15-2347) AND 6 (DF15-2368) 46
FIGURE 28. CARBON FOIL GAUGE DATA AND CALCULATIONS, TARGET TEST 10 (K3-1304) 47
FIGURE 29. TARGET TEST 4 (DF15-2330), RADIAL PINDUCER 4, EXPERIMENTAL AND CALCULATED DATA 48
FIGURE 30. TARGET TEST 5 (DF15-2347), PINDUCER 2, EXPERIMENTAL AND CALCULATED DATA 49
FIGURE 31. TARGET TEST 5 (DF15-2347), PINDUCER 3, EXPERIMENTAL AND CALCULATED DATA 49
FIGURE 32. TARGET TEST 6 (K3-2368), PINDUCER 2, EXPERIMENTAL AND CALCULATED DATA 50
FIGURE 33. TARGET TEST 7 (K3-1235), PINDUCER 3, EXPERIMENTAL AND CALCULATED DATA 50
FIGURE 34. TARGET TEST 9 (K3-1290), PINDUCER 3, EXPERIMENTAL AND CALCULATED DATA 51
FIGURE 35. TARGET TEST 10 (K3-1304), PINDUCER 3, EXPERIMENTAL AND CALCULATED DATA 51
FIGURE 36. POWER LAW CRITERION PREDICTIONS FOR VARIOUS PROJECTILE RADII .. 52
FIGURE 37. CALCULATED PRESSURE AT IGNITION CRITERION, WORST-CASE LOCATION, TARGET TEST 5 (DF15-2347) 53

PBX 9501 HIGH EXPLOSIVE VIOLENT RESPONSE/ LOW AMPLITUDE INSULT PROJECT: PHASE I

by

D. J. Idar, R. A. Lucht, R. Scammon, J. Straight, and C. B. Skidmore

ABSTRACT

Preliminary modeling and experimental analyses of the violent reaction threshold of semi-heavily confined PBX 9501 to low velocity impact have been completed. Experimental threshold measurements were obtained with ten tests using a spigot gun design to launch a hemispherical projectile at the high explosive contained in stainless steel. Powder curves were determined for several gun barrel designs, powders, and projectile materials and have proven to be very reproducible over the range of 75 to 325 ft/s. A threshold velocity of approximately 246 ft/s for violent reaction of the PBX 9501 was determined with experimental gauge and switch measurements and the remaining physical test evidence. Preliminary analyses of the PBX 9501 samples retrieved from both unreacted and partially reacted targets have been completed. Core samples were obtained from the unreacted targets and submitted for density determinations. The subsequent analysis supports the concept that the PBX 9501 yields and fractures under the low velocity compression event to expand and fill the annular gap in the target design. Samples of PBX 9501 from the partially reacted targets were examined with scanning electron microscope and light microscope techniques. Increased evidence of mechanical twinning effects are noted in the HMX crystals from the partially reacted targets. Finite element calculations using DYNA2D, with a modified ORION post processor, without reaction or chemistry models, were used to support the design of targets, to compare predictive analyses with experimental measurements, and to evaluate a proposed ignition criterion in a power law form for threshold to reaction with dependence on pressure, maximum shear strain rate, and time variables. The calculations show good agreement with the physical dent and deformation data from the remaining target evidence; however, they do not match the experimental pressure gauge measurements well. The differences can be attributed to a combination of the experimental variables, the need for better materials properties values in the calculations, and the need for chemistry and reaction in the predictions. Also, further evaluation of the ignition criterion form is needed to account for the probability of fracture in the PBX 9501.

I. INTRODUCTION

Strong shock-to-detonation-transition (SDT) of high explosives (HE) has been well characterized over several decades in shock wave physics research and finite element and hydrodynamic code analyses. These initiation mechanisms are normally associated with impacts of relatively high velocities, ≥ 1 mm/μs, and pressures, ≥ 10 kbars. More recently, the focus of energetic materials research has shifted to determining, defining, and predicting the phenomena associated with relatively weak, low amplitude insults and the probability for violent reaction leading to property damage and casualties.

These HE safety concerns are focused on the storage, handling, transport, and inadvertent initiation of conventional and nuclear weapons, and methods related to disposal, dismantlement, and replacement. Examples of these events include the impact experienced by a weapon if it is accidentally dropped, or the collision of a projectile with a weapon in storage or transport. Under these conditions the potential exists to either sensitize the HE or to produce a violent reaction with a possible loss of life and property. The goal is to identify the relevant parameters: mechanical, chemical, confinement, and impact conditions that lead to sensitization, initiation, and/or violent reaction of the HE. This knowledge will assist in the development and verification of our predictive code capabilities. This knowledge will be used to establish and modify those methods associated with the safety issues.

PBX 9501, a LANL formulation, was chosen for our research because it represents a large portion of the HE in the remaining nuclear stockpile. It is a 95.0/2.5/2.5 wt % HMX/Estane/BDNPA-BDNPF formulation[1] with a theoretical maximum density (TMD) of 1.860 g/cm^3 and a nominal detonation velocity of 8.83 mm/μsec. The average density of the samples used for the research reported here was 1.837 g/cm^3 (~98.7% TMD).

The LLNL DYNA2D finite element code was chosen to support the modeling effort. This included experiment design calculations, material model development, and analysis of the experimental results. This code was also used to investigate the PBX 9501 ignition criterion developed by Richard Browning.

II. BACKGROUND

Recently Steven Chidester et al.[2] reported on their experimental and theoretical DYNA2D analyses of low pressure impacts on the explosives LX-10-1 and LX-17-0. Their methodology, based on frictional work for ignition, was used to predict the projectile threshold velocity to produce a violent event in the LX-10-1. However, they were unable to obtain a reaction in the LX-17 under their experimental conditions.

The explosive LX-10-1 is a LLNL formulation with 94.5/5.5 wt % HMX/Viton A[3] with a TMD of 1.895 g/cm^3 and a nominal detonation velocity of 8.85 mm/μs. The critical temperatures of LX-10-1 and PBX 9501 are essentially the same, 215°C, and the drop weight impact heights differ little. However, they do differ in their skid, Susan, and spigot test (a different test than described in this report) results, with LX-10-1 showing more sensitivity. For their research, Chidester and coworkers used LX-10-1 samples with an average density of 1.86 g/cm^3 (≈98.2% TMD).

The explosive LX-17-0 is also a LLNL formulation with 92.5/7.5 wt % TATB/Kel-F 800 with a TMD of

1.944 g/cm^3 and a nominal detonation velocity of 7.63 mm/μs. The average density of their samples was 1.90 g/cm^3 (~97.7% TMD).

For their impact tests, Chidester et. al. employed a 2.56 kg, hemispherical nose, tantalum (Ta) projectile with a 0.46 kg sabot launched from a smooth bore 76-mm diam. gas gun at a LX-10-1, metal encased, plane geometry target. They measured v_{50} values for this arrangement ranging from ~106.0–115.8 ft/s (32.3–35.3 m/s), which produced explosions. For comparison, a velocity of 1750 ft/s (533 m/s) is required to produce an SDT 0.5-in. run-to-detonation in PBX 9501 with a flat, mild steel plate impact based on 1-D Hugoniot[3] matching calculations and the PBX 9501 Pop plot. Significantly higher velocities would be required for SDT driven by a hemispherical impactor because the shock waves produced would be highly divergent. Similar tests by Chidester et. al. on LX-17-0 encased targets and with a projectile velocity as high as 463.3 ft/s (141.2 m/s) did not produce a violent reaction.

III. EXPERIMENTAL

A. Spigot Gun, Projectile Description, and Powder Curve Tests

The projectile characteristics required by this project were a 2 kg projectile of arbitrary size and shape traveling at velocities from 75 ft/s to 325 ft/s (≈22 to 100 m/s). The arbitrary size and shape limited the utility of a conventional projectile-in-tube launch system, which would have required an elaborate sabot design and a massive sabot stripper. Although a gas driven system would have worked well for the 75 ft/s, it would have had trouble achieving the 325 ft/s needed.

For these reasons, a powder gun driving a spigot projectile was designed with the use of either BLC2 or IMR 4350 rifle powder. A small bore diameter was needed to burn the gunpowder reliably at high pressures. A small bore diameter and short barrel were also needed to achieve the very low 75 ft/s. The initial design had a 0.5-in. diam. bore with a 9-in. long barrel. For simplicity, a rimmed rifle cartridge (.45-70 cal.) is used. A 1.5-in. long polyethylene obturator is used to seal the powder gas products. The projectile has a head of arbitrary size and shape driven by a 0.5-in. diam. by 5.25-in. long shank (spigot). The current projectile has a 3-in. diam. hemispherical nose, is made of cold rolled mild steel, and has a total mass (with spigot) of 2 kg. The gases are vented before the projectile leaves the bore to reduce tip-off. This gun worked well at low velocities, but the spigot buckled in-bore at higher velocities. Thus, the design was modified to a 0.75-in. bore still using the 0.45-70 cal cartridge. The new barrel has a 2-in. OD and is made of mild steel. The receiver or breech block has a 4-in. OD and is also made of mild steel. The barrel screws into the breech block with an Acme thread.

Because the projectile is so massive (compared to normal rifle bullets), the powder burns almost as if it was in a closed container. As such, the burn characteristics do not match any published data, and computer code predictions are of little value. Thus, we have made some attempts to measure the burn pressure using piezoelectric pressure transducers. We have consistently overranged the 100,000 psi (~689 MPa) transducers and have, on several occasions, literally blown them out the side of the barrels. We hope to pursue these pressure measurements next year. Even with the 0.75-in. diam. spigot, we see plastic deformation of the base of the spigot at velocities above ~250 ft/s. We have achieved over 300 ft/s using hardened spigots. In an attempt to reach 330 ft/s, we ruptured a barrel. Higher velocities required a thicker, higher strength barrel. At this time, the powder weight vs. velocity curve for the 2-in. barrel is well established, and the gun is performing reliably. A total of 71 tests has been fired with the 0.75-in. bore gun. Different barrels have slightly different powder curves due to small manufacturing variances.

A higher pressure barrel has been designed and fabricated, and initial testing has been completed. The

barrel has a 3-in. OD, is made of AISI 4340 steel heat treated to Rockwell hardness range "c" (Rc) 35, and uses a 0.45-basic cartridge. The breech block has a 6-in. OD. The 0.45-basic cartridge is about 1 in. longer than the 0.47-70 that we use with the 2-in. barrel. The extra length has two effects. The first, of course, is to allow us to use more powder. The second effect is that we have more ullage and, thus, a significant shift in the powder weight vs. velocity curve. Because we are operating at extremely high pressures, we are using strain gauges to measure the pressure history. Hoop and axial strain gauges are mounted on the barrel over the chamber. An example of the strain measurement is shown in Figure 1. The two measurements can be combined to compute the bore pressure as a function of time. This is shown in Figure 2. The peak pressure in this test was 154,000 psi (~1.07 GPa). A gun barrel is neither a closed cylinder nor an open one. One might expect the axial strain to lie between these two conditions (tensile and a fixed fraction of the hoop strain). As can be seen in Figure 1, the axial strain clearly does not conform to these expectations. The strain starts out negative (compressive) and then oscillates with a high amplitude. The initial compression is due to the Poisson effect combined with the undefined end conditions. The initial local contraction of the material then excites the fundamental mode of axial vibration, and the barrel begins to oscillate. This explanation was verified by comparing a Fast-Fourier-Transform (FFT) of the axial strain gauge data with a finite element analysis of the entire gun assembly. All of the FFT analyses show a strong peak at 2 kHz, which correlates with the fundamental mode of vibration from the finite element analysis.

We have completed a total of 12 tests with the high pressure gun. Of these, 6 included strain gauges; however, data were collected on only three because of recording difficulties. One of the tests was the highest velocity possible and at a live target. We achieved 325 ± 5 ft/s.

Because of the short barrels on all of these guns, a relatively flexible gun mount, and the very forceful recoil, the projectile hit point varies considerably from test to test. It is often up to 1-in. high in 6 ft of flight, and varies from 1-in. left to 1-in. right of the aim point. To achieve better hit accuracy, later tests were performed by moving the gun to within 4 ft of the target. Targets that reacted violently usually damaged the barrel.

For safety reasons, no arming energy is permitted on the firing mound until all personnel are safely inside

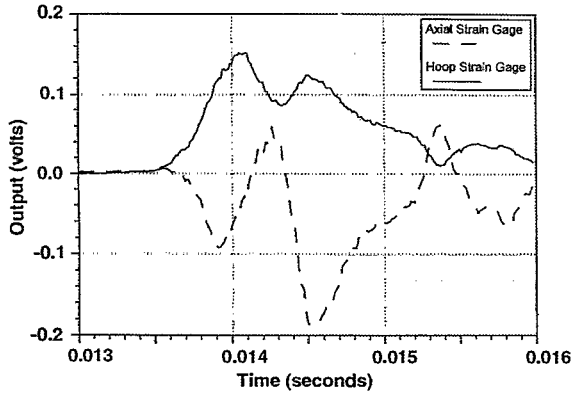

Figure 1: Hoop and axial strain measurements obtained from the high pressure barrel design for the spigot gun.

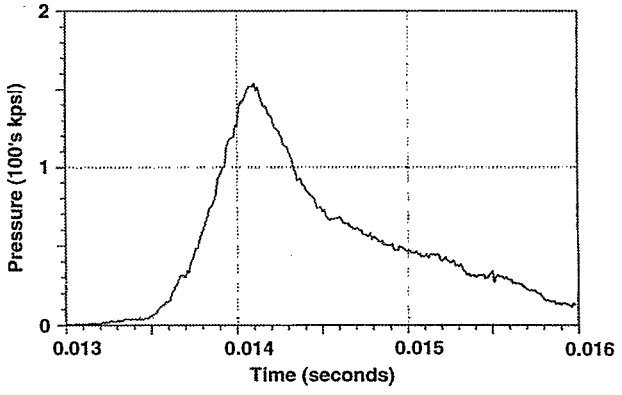

Figure 2: Bore pressure as a function of time for the high pressure barrel design.

the bunker. Thus, an electrically actuated, pneumatically driven firing mechanism was designed. The final electrical and compressed air connections are made from inside the bunker after the area is cleared.

One of the most important performance characteristics of the gun is the projectile velocity. Because most of the powder gases are vented before the spigot leaves the muzzle, a velocity measurement can be made very close to the muzzle. Because of the proximity of the gun to the target, any instrumentation on the gun, target, or between the two would be vulnerable to target detonation. An inexpensive, easily replaceable light/photodiode system was designed by Bob Critchfield to determine the projectile velocity. It is composed of three sets of halogen lights and photodiodes spaced at 3-in. intervals in a wooden frame. The photodiode outputs are recorded on digital oscilloscopes. The three profiles yield two independent velocity measurements. An average velocity was then determined from these two values, and this value is reported with the powder curve results and the live target test results. A photograph of the spigot gun with a light/photodiode system is shown in Figure 3, and the performance data are given in Tables 1 and 2.

B. Inert Target Description

The inert targets were built with multiple layers of 0.5 to 1.0-in. thick plywood sandwiched together with staples or nails. The inert targets were used to verify aiming for the gun, to establish the powder curve, and to test the triggering mechanisms for the diagnostics. Crosshairs were drawn on the targets to determine the impact accuracy.

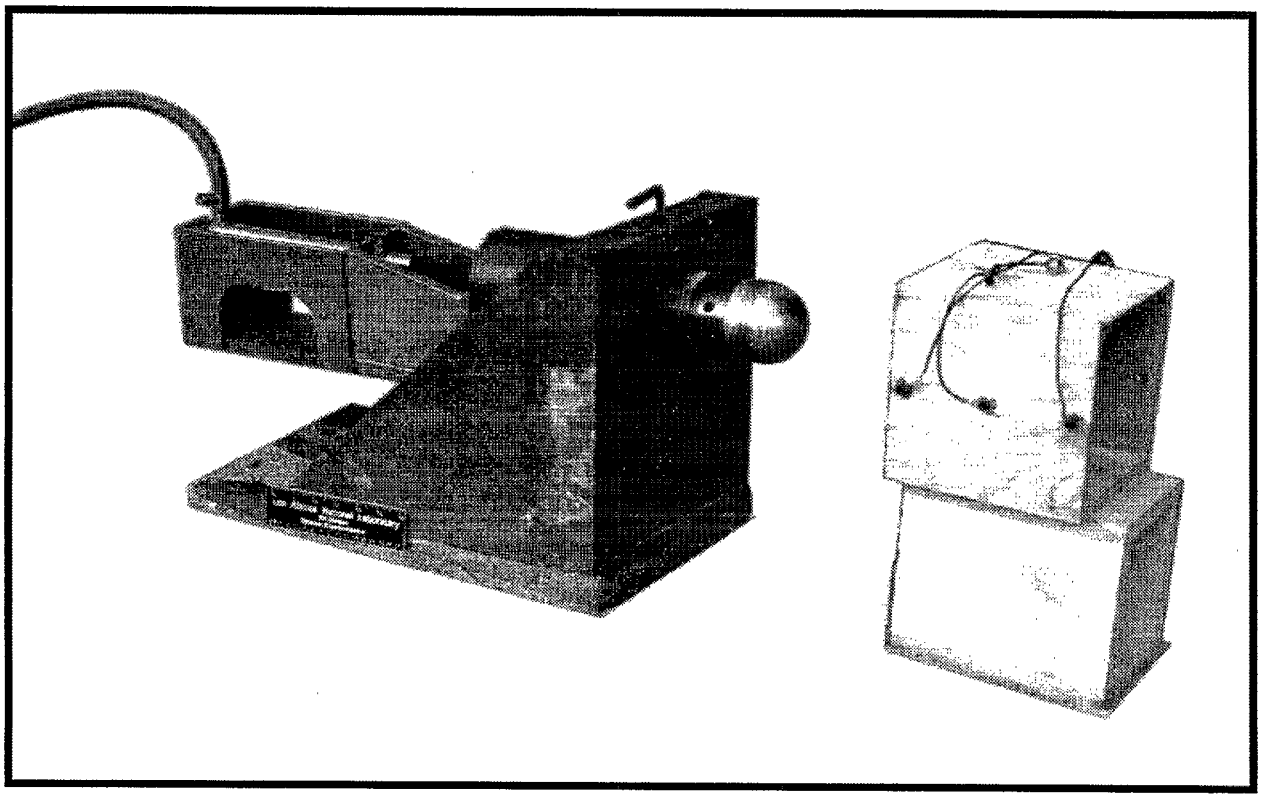

Figure 3: Spigot gun and photodiode velocity screen box.

Table 1. Powder curve performance results for low pressure barrel design (BLC2).

TEST #	Powder Wt. (g)	Velocity (ft/s)	Comments
DF15-548	2.0	104.038	old obturator
DF15-549	2.5	115.989	
12/14/94	2.75	no velocity data	primer burned only, below freezing temp.
12/14/94	2.75	no velocity data	primer burned only, below freezing temp.
12/14/94	2.75	no velocity data	primer burned only, below freezing temp.
DF15-550	3.0	152.932	
DF15-581	3.0	184.68	
DF15-551	3.5	208.15	
DF15-582	3.5	205.281	
DF15-583	3.5	231.84	new obturator
DF15-2364	3.5	234.95	impact 1-in. high, new obturator
DF15-584	4.0	240.493	
DF15-552	4.0	227.025	
DF15-2365	4.0	256.00	estimated impact 1-in. high
DF15-2366	4.0	255.31	impact 1-in. high, new obturator
DF15-587	4.001	236.748	
DF15-2350	4.5	269.01	impact 1.25-in. high, new obturator
DF15-2351	4.5	265.726	impact 0.75-in. high, new obturator
DF15-585	4.5	no velocity data	transducer blowout
DF15-642	4.507	256.714	
DF15-586	5.0	no velocity data	transducer blowout
DF15-644	5.0	264.575	new barrel, new obturator
DF15-803	5.0	no velocity data	new barrel
DF15-643	5.003	no velocity data	old obturator- transducer blowout
DF15-2345	5.261	264.84	impact 1-in. high, new obturator
DF15-2346	5.261	no velocity data	impact 1.25-in. high, new obturator
DF15-2347	5.261	264.939	new obturator
DF15-2318	5.261	269.266	impact 1.5-in. high
DF15-2319	5.261	278.589	
DF15-2317	5.262	267.241	impact 1.5-in. high
DF15-2376	5.325	308.8	impact 0.5-in. high, 1.0-in. left, new obturator
DF15-2377	5.325	310.4	impact 0.5 -in. high, 1.0-in. left, new obturator
DF15-665	5.425	no velocity data	barrel blowout
DF15-2384	5.44	no velocity data	barrel blowout

Table 1. Powder curve performance results for low pressure barrel design (IMR4350).

Test #	Powder Wt. (g)	Velocity (ft/s)	Comments
DF15-2326	1.25	95.222	impact 0.5-in. high, old obturator
DF15-2327	1.25 + cow	128.275	impact 0.5-in. right, 0.25-in. high, new obturator, cow ≡ excess case volume was filled with cream of wheat
DF15-2323	2.75	189.998	impact on crosshairs, old obturator
DF15-2324	2.75	188.868	impact 0.5-in. high, old obtrurator
DF15-2325	2.75	185.556	impact 1-in. high, old obturator
DF15-2328	3.25	no velocity data	impact 1-in. high, new obturator
DF15-2329	3.25	218.521	impact 1-in. high,0.5-in. left, new obturator
	3.25	214.94	impact 0.375-in. high, 0.375-in. left
DF15-2367	3.4	234.9	impact 1-in. high, new obturator
DF15-2368	3.4	232.6	impact 0.5-in. high, new obtrurator
DF-2358	3.5	no velocity data	impact 1-in. high, new obturator
DF-2359	3.5	237.91	impact 1-in. high, 0.75-in. left, new obturator
DF-2364	3.5	234.95	impact 1-in. high, new obturator
K3-1238	3.6	244.5	impact 0.5-in. low, 1- in.right
K3-1277	3.6	241.75	0.5-in. low, 5-in. left [1]
K3-1278	3.6	236.96	0.5-in. high, 0.125-in. left [1]
K3-1286	3.7	243.996	[1]
K3-1287	3.7	245.151	[1]
K3-1290	3.7	246.345	target exploded, barrel destroyed
K3-1136	3.8	255.95	impact 1-in. left [1]
K3-1237	3.8	251.85	impact 0.5-in. high, 1-in. left [1]
DF15-2401	3.9	252.525	impact 0.875-in. high, 1.25-in. left
DF15-2402	3.9	250.627	impact 1.25-in. high, 0.875-in. left
K3-1135	3.9	no velocity data	impact 1.5-in. high
K3-1140	3.9	no velocity data	impact 0.75-in. high
K3-1174	3.9	251.256	impact on crosshairs
K3-1182	3.9	252.8	impact 0.5-in. high, 1.5-in. left [1]
K3-1183	3.9	242.7	impact 0.5-in high, 0.25-in left, spiked tip projectile

[1] Optical sight was adjusted between tests, thus the hit point data is of little significance.

Table 1. Powder curve performance results for low pressure barrel design (IMR4350 cont.).

Test #	Powder Wt. (g)	Velocity (ft/s)	Comments
K3-1233	3.9	248.76	impact 0.25-in. high, 0.25-in. left, spiked tip projectile
K3-1234	3.9	246.3	impact on crosshairs, spiked tip projectile
K3-1235	3.9	no velocity data	target exploded, barrel destroyed [1]
DF15-2360	4.0	252.57	impact 1-in. high, new obturator
DF15-2361	4.0	249.23	impact 1-in. high, new obturator
DF15-2382	4.0	256.7	impact 0.5-in. high, 1-in. right, new obturator
DF15-2383	4.0	253.9	impact 0.75-in. high, 1.0 in left, new obturator
DF15-2362	4.5	274.65	impact 1-in. high, new obturator
DF15-2363	4.5	271.48	impact 1.25-in. high, new obturator

[1] Optical sight was adjusted between tests, thus the hit point data is of little significance.

C. Live Target I Description

The original target design was based on a modification of the target assembly used by Chidester et. al.[2] with the following modification: ten target assemblies have been machined from 304 ss according to the scales and dimensions given in Clinton Shonrock's drawing number 139Y-600005,[4] consisting of a holder, disc, and retaining ring. Both the holder and retaining ring are machined with eight evenly dispersed holes to allow for assembly of the target. The PBX 9501 and Sylgard 184 potting articles were also manufactured according to the same drawing descriptions, with diameters of 5.75-in. each, and thicknesses of 1.00-in. and 0.020-in, respectively. The stainless steel cover disc was nominally 0.125 ± 0.001-in. thick with a flatness of 0.002-in. across the 5.75-in. diam. Densities were determined for each of the PBX 9501 articles, with an average density of 1.837 g/cm^3. The density information for each HE article is provided in Table 3. Assembly of the targets was performed by ESA personnel at TA-16, Bldg. 410, according to the assembly procedures written by either Ron Flury or Dick Scammon. The original design dimensions allowed for an annular gap of 0.125-in. between the HE O.D. and the holder I.D. Figure 4 is a schematic of the target design I. Seven 1/2-13 hex nuts and bolts are used to secure the holder, the PBX 9501 piece, the Sylgard 184, the disc cover, and the retaining ring together. The eighth hole is used to secure the assembly to the mild steel backing plate described below. Four assemblies, targets 1–4, were assembled in this fashion and used for the first four spigot gun tests.

Table 2: Powder curve performance results for high pressure barrel design (IMR4350).

Test #	Powder Wt. (g)	Velocity (ft/sec)	Comments
K3-1288	3.5	no velocity data	impact 1.5-in. high[1]
K3-1289	4.0	241.26	impact 1.5-in. high[1]
K3-1336	4.5	252.8	impact 1.5-in. high[1]
K3-1337	5.0	271.0	impact 1.5-in. high[1]
K3-1339	5.0 + cow	291.7	impact 0.25-in. high, 1.0-in. left, cow ≡ excess case volume was filled with cream of wheat [1]
K3-1338	5.5 + cow	285.47	[1]
K3-1340	5.5 + cow	302.4	impact 1.0-in. high[1]
K3-1341	6.0	282.9	[1]
K3-1342	6.5	319.8	141,200 psi chamber pressure [1]
K3-1343	7.0	no velocity data	152,500 psi chamber pressure [1]
K3-1344	7.0	325.75	154,000 psi chamber pressure [1]
K3-1304	7.0	no velocity data	(1)

[1] Optical sight was adjusted between tests, thus the hit point data is of little significance.

Table 3: PBX 9501, lot number HOL96C73 1, density report. All measurements were determined at 73.00°F.

Piece Number	Dry Wt. (g)	Wet Wt. (g)	Volume (cm^3)	Density (g/cm^3)
45614-0001	780.10	356.20	424.923	1.836
45614-0002	780.30	356.50	424.823	1.837
45614-0003	780.50	356.70	424.823	1.837
45614-0004	780.30	356.30	425.023	1.836
45614-0005	780.70	356.60	425.123	1.836
45614-0006	780.90	356.80	425.123	1.837
45614-0007	780.70	356.30	424.422	1.837
45614-0008	780.50	356.70	424.823	1.837
45614-0009	780.10	356.50	424.622	1.837
45614-0010	780.20	356.30	424.923	1.836